2021 43rd Annual International Conference of the
IEEE Engineering in Medicine & Biology Society (EMBC)
Oct 31 - Nov 4, 2021. Virtual Conference

Towards Characterization of the Complex and Frequency-dependent Arterial Compliance based on Fractional-order Capacitor

Mohamed A. Bahloul, *Member, IEEE,* Yasser Aboelkassem *Member, IEEE,*
and Taous-Meriem Laleg-Kirati, *Senior Member, IEEE*

***Abstract*—Arterial compliance is a vital determinant of the ventriculo-arterial coupling dynamic. Its variation is detrimental to cardiovascular functions and associated with heart diseases. Accordingly, assessment and measurement of arterial compliance are essential in the diagnosis and treatment of chronic arterial insufficiency. Recently, experimental and theoretical studies have recognized the power of fractional calculus to perceive viscoelastic blood vessel structure and biomechanical properties. This paper presents five fractional-order model representations to describe the dynamic relationship between the aortic blood pressure input and blood volume. Each configuration incorporates a fractional-order capacitor element (FOC) to lump the apparent arterial compliance's complex and frequency dependence properties. FOC combines both resistive and capacitive attributes within a unified component, which can be controlled through the fractional differentiation order factor, α. Besides, the equivalent capacitance of FOC is by its very nature frequency-dependent, compassing the complex properties using only a few numbers of parameters. The proposed representations have been compared with generalized integer-order models of arterial compliance. Both models have been applied and validated using different aortic pressure and flow rate data acquired from various species such as humans, pigs, and dogs. The results have shown that the fractional-order framework is able to accurately reconstruct the dynamic of the complex and frequency-dependent apparent compliance dynamic and reduce the complexity. It seems that this new paradigm confers a prominent potential to be adopted in clinical practice and basic cardiovascular mechanics research.**

***Keywords*—Fractional calculus, fractional-order capacitor, apparent compliance, aortic input impedance.**

I. Introduction

Cardiovascular diseases (CVDs) are the number one cause of premature death worldwide. Besides, decreased arterial compliance is recognized to be detrimental to the heart and arterial functions [1]. The variation in arterial compliance is associated with major forms of CVDs, mainly hypertension and atherosclerosis [2]. Accordingly, assessment and evaluation of arterial compliance changes are crucial in diagnosing and treating hemodynamic disorders. Commonly, vascular compliance stands for the ability of the vessel to store the blood. Functionally, arterial compliance can be defined as the ratio of an incremental variation in the blood volume (dV) due to an incremental variation in distending pressure (dP). Mathematically it can be expressed as: $C = dV/dP$. Several analytical and experimental studies focused on modeling arterial compliance [3].

A century ago, with the introduction of the well-known linear Windkessel representation of the arterial system, the arterial compliance was assumed to have a single constant value for the entire cardiac cycle and hence the transfer function relating the variation of the blood volume to the blood pressure input changes was considered to be a constant as well. Accordingly, the arterial compliance was modeled within the arterial Windkessel model as an ideal capacitor whose capacitance is constant [4], [5]. However, this assumption was not realistic, and its drawbacks were reflected essentially in the estimation of the hemodynamic. In fact, it does not lead to the correct evaluation of the true value of arterial compliance. Besides, by analyzing the transfer function blood Volume/input pressure, experimental studies have shown that this relationship is frequency-dependent, and a time delay between the arterial blood volume and the input blood pressure coexist. Hence a variation in the arterial compliance along the cardiac cycle is expected [6]. In order to take into account this frequency dependency, some research proposals have promoted a new configuration where they considered the viscoelastic properties of the arterial vessel model and modeled the arterial compliance using the so-called Voigt-cell configuration. This type of arterial model was known as Viscoelastic Windkessel. Although the viscoelastic *Voigt-cell* has resolved some contradictions of the standard elastic Windkessel, this configuration does present some limitations as it does not account for the stress-relaxation experiments [5]. Experimenters have proposed using high-order viscoelastic configurations to overcome this restriction by connecting many Voigt-cell, for example. This solution might accurately model the whole arterial compliance and its feature; however, it is considered a very complex alternative that poses extra challenges. Indeed, for higher-order models, the number of parameters to identify is more significant, while the collected real data is small and insufficient. It is also recognized that

Mohamed A. Bahloul and Taous-Meriem Laleg-Kirati are with the Computer, Electrical and Mathematical Sciences and Engineering Division (CEMSE), King Abdullah University of Science and Technology (KAUST), Thuwal 23955-6900, Makkah Province, Saudi Arabia. E-mail:{mohamad.bahloul, taousmeriem.laleg}@ kaust.edu.sa
Yasser Aboelkassem is with College of Innovation and Technology, University of Michigan-Flint, MI 48502, USA. E-mail: yasser@vt.edu

reduced-order models are desirable for their simplicity and ease of exploration [7].

In the last decades, non-integer differentiation, the so-called fractional-order differential calculus, became a popular tool for characterizing real-world physical systems and complex behaviors from various fields such as biology, control, and electronics, and economics. The long-memory and spatial dependence phenomena inherent to the fractional-order systems present unique and attractive peculiarities that raise exciting opportunities to represent complex phenomena that represent power-law behavior accurately [8]–[10]. Regarding cardiovascular system modeling, the power-law behavior has been proved in the viscoelasticity characterization of an elastic aorta. The *in-vivo* and *in-vitro* experiment have shown that fractional-order calculus tools are more convenient to precisely represent the dynamic arterial; the viscoelasticity properties of the collagenous tissues in the arterial bed; the arterial blood flow [11], [12]; red blood cell (RBC) membrane mechanics [13] and the heart valve cusp [12], [14]–[16]. Recently, we adopted fractional-order derivative tools to the well-known arterial Windkessel paradigm by substituting the ideal capacitor, which accounts for the total arterial compliance, with a fractional-order capacitor, [7], [17], [18]. Our preliminary investigation confirmed that the fractional-order impedance is the right candidate for the accurate assessment of the aortic input impedance. Moreover, a strong correlation between the main hemodynamic determinants and the fractional differentiation order (α) has been proved. [19], [20]. The fractional order is used to describe the transition between viscosity and elasticity more accurately.

This paper presents five fractional-order model representations to describe the dynamic relationship between the aortic blood pressure input and blood volume. Each configuration incorporates a fractional-order capacitor element (FOC) to lump the apparent arterial compliance's complex and frequency dependence properties. FOC combines both resistive and capacitive attributes within a unified component, which can be controlled through the fractional differentiation order factor, α. Besides, the equivalent capacitance of FOC is by its very nature frequency-dependent, compassing the complex properties using only a few numbers of parameters. The proposed representations have been compared with generalized integer-order models of arterial compliance. Both models have been applied and validated using different aortic pressure and flow rate data acquired from various species such as humans, pigs, and dogs.

II. Background

A. Apparent Compliance

The apparent compliance, C_{app}, refers to the arterial bed's capacity to store blood dynamically. Functionally, it corresponds to the transfer function between the blood volume (V) and input blood pressure (P_{in}). In the following, we present its mathematical derivation:

Based on the conservation of mass, the arterial blood flow pumped from the heart to the arterial vascular bed (Q_{in}) can be expressed as:

$$Q_{in} = Q_{stored} + Q_{out}, \tag{1}$$

where Q_{stored} is the blood stored in the arterial tree, and Q_{out} corresponds to the flow out of the arterial system. In the frequency domain Q_{out} can be expressed as:

$$Q_{out}(w) = \frac{1}{R_{app}(\omega)} P_{in}(w). \tag{2}$$

where ω corresponds to the angular frequency and R_{app} is the apparent arterial resistance [3]. Q_{stored} is defined as the rate of flow by taking the first derivative of the volume equation for the time.

$$Q_{stored}(t) = \frac{dV}{dt} = \underbrace{\frac{dV(t)}{dP_{in}(t)}}_{C_{app}} \frac{dP_{in}(t)}{dt}, \tag{3}$$

Hence in the frequency domain Q_{stored} can be expressed as:

$$Q_{stored} = j\omega P_{in} C_{app} \tag{4}$$

Aortic input impedance Z_{in} describes the ability of the arterial system to hamper the blood flow dynamically. Functionally, Z_{in} is defined as the dynamic relationship, in the frequency domain, of the arterial blood pressure (P_{in}) and blood flow (Q_{in}) at the entrance of the systemic circulatory system, that is:

$$Z_{in}(\omega) = \frac{P_{in}(\omega)}{Q_{in}(\omega)}, \tag{5}$$

Substituting equations (2) and (4) into equation (1) gives:

$$Q_{in} = j\omega P_{in} C_{app} + \frac{1}{R_{app}(\omega)} P_{\omega}(w). \tag{6}$$

Rearranging the above equation yields an expression for C_{app} in terms of Z_{in} and R_{app} as follow:

$$C_{app} = \frac{R_{app} - Z_{in}}{j\omega R_{app} Z_{in}} \tag{7}$$

B. Fractional-order capacitor

Fractional-order capacitor is a constant phase element [21]. It is an electrical element that represents a fractional-order derivative relationship between the current, $Q(t)$, passing through and the voltage, $P(t)$, across it with respect to time, t, as follow:

$$Q(t) = C_{\alpha} \frac{d^{\alpha}}{dt^{\alpha}} P(t), \tag{8}$$

where C_{α} is a proportionality constant so-called pseudo-capacitance, expressed in units of $[\mathrm{Farad}/\mathrm{second}^{1-\alpha}]$. The conventional capacitance, C, in unit of Farad is related to C_{α} as $C = C_{\alpha}\omega^{\alpha-1}$ that is frequency-dependent. The fractional-order impedance (Z_{α}) is expressed as follow:

$$Z_{\alpha}(s) = \frac{1}{C_{\alpha} s^{\alpha}} = \underbrace{\frac{1}{C_{\alpha}} \omega^{-\alpha} \cos(\phi)}_{Z_r} - j \underbrace{\frac{1}{C_{\alpha}} \omega^{\alpha} \sin(\phi)}_{Z_i}, \tag{9}$$

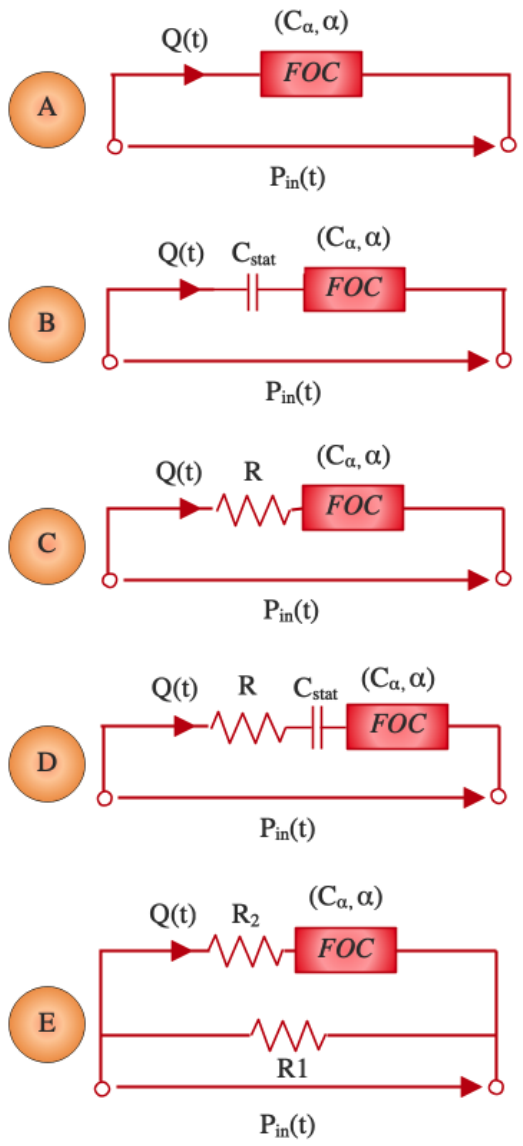

Fig. 1: Schematic representations of the electrical analogue of the proposed fractional-order models.

where s corresponds to the *Laplace* variable and ϕ denotes the phase shift given by the formula: ϕ=$\alpha\pi/2$ [rad] or ϕ=90α [degree or °]. Z_r and Z_i are the real and imaginary parts of Z_α corresponding to the resistive and capacitive portions, respectively. From (9), it is apparent that the transition between resistive and capacitive parts is ensured by α. If $0 \leq \alpha \leqslant 1$, the bounding conditions of α will corresponds to the discrete conventional elements: the resistor at $\alpha = 0$ and the ideal capacitor at $\alpha = 1$). As α goes to 0, (Z_i) convergence to 0, and thus the fractional element looks like that a pure resistor, whereas as α goes to 1, (Z_r) converges to 0 and hence, the fractional element serves as a pure capacitor. Bearing these properties in mind, it is clear that the fractional order α parameter allows extra versatility.

III. Models

As shown in the previous section, the FOC offers extra flexibility via its fractional differentiation order α, and it permits the smooth transition and control between the resistive and capacitive parts, which might be investigated to model the arterial system properties. By rewriting (3) in the fractional-order domain as:

$$Q_{stored}(t) = \frac{d^\alpha V}{dt^\alpha} = \underbrace{\frac{d^\alpha V(t)}{d^\alpha P_{in}(t)}}_{C_{\alpha_{app}}} \frac{d^\alpha P_{in}(t)}{dt^\alpha}, \tag{10}$$

we found that FOC can be a great candidate to present the complex and frequency-dependent dynamic of the arterial compliance. In fact, based on (10) the pseudo compliance, $C_{\alpha_{app}}$, should be expressed in the unit of $[\mathrm{l/mmHg\ .sec}^{1-\alpha}]$ that makes, by its very nature, the conventional compliance (C_C), in the unit of $[\mathrm{l/mmHg}]$, frequency-dependent as:

$$C_C = C_{\alpha_{app}}(j\omega)^{\alpha-1}. \tag{11}$$

Hence FOC has a physical foundation in representing the complex and frequency dependence of the apparent compliance. Besides, based on the value of α, the real and the imaginary parts of the resultant FOC's impedance can have different levels, so by analogy, α can control dissipative and storage mechanisms, and so the viscous and elastic part of the arterial wall. It is worth noting that the equivalent analog circuit of FOC can be viewed as infinity Voigt-cells connected in parallel [22], [23]. Hence, FOC might lead to a minimal representation of the arterial network's mechanical properties using only two parameters (α and C_α). In the following, we present the five fractional-order representations of arterial compliance. The analog structures of the proposed models are shown in Fig. 1. The fractional-order representations have been compared with generalized integer-order models of arterial compliance that are presented as well.

A. Fractional-order Models

1) Model A: It comprises only one single FOC. As detailed in the previous sections, the apparent compliance expressed in unit of $[\mathrm{l/mmHg}]$ can be written as:

$$C_c^A = C_\alpha(j\omega)^{\alpha-1}. \tag{12}$$

2) Model B: It comprises an ideal capacitor (C_{stat}) accounting for the static compliance and FOC connected in series. The apparent compliance expressed in the unit of $[\mathrm{l/mmHg}]$ can be written as:

$$C_c^B = \frac{C_\alpha C_{stat}(j\omega)^\alpha}{C_\alpha(j\omega)^\alpha + C_{stat}(j\omega)}. \tag{13}$$

3) Model C: It comprises a resistor (R) and FOC connected in series. The apparent compliance expressed in the unit of $[\mathrm{l/mmHg}]$ can be written as:

$$C_c^C = \frac{C_\alpha(j\omega)^{\alpha-1}}{1 + RC_\alpha(j\omega)}. \tag{14}$$

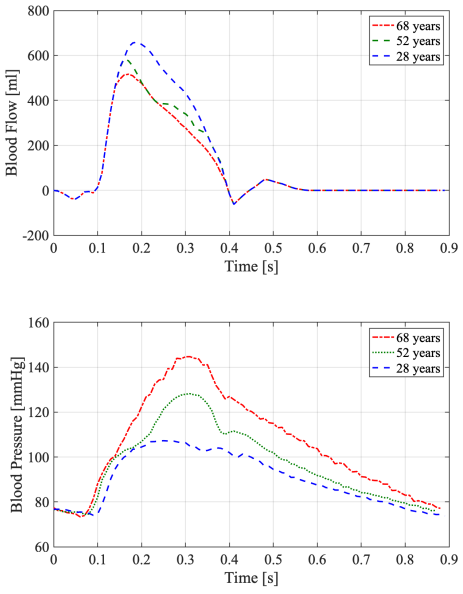

Fig. 2: *In-vivo* human aging data sets digitized from (Nichols et al., [24]). It presents the blood flow rate and pressure waveforms at different ages, namely 28, 52, and 68 years.

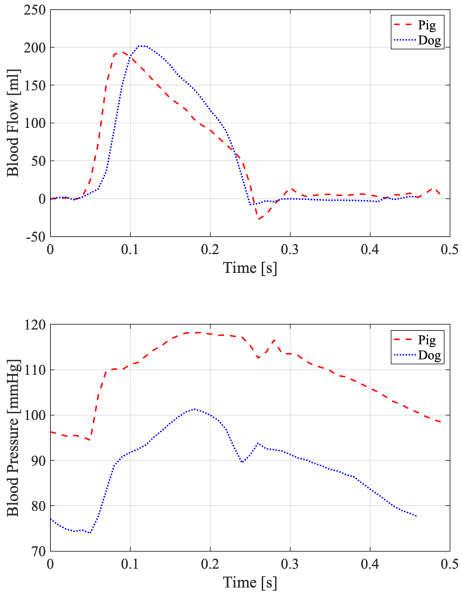

Fig. 3: *In-vivo* animal (Pigs and Dogs) data sets digitized from (Segers et al., [26]).

4) Model D: It comprises a resistor (R), an ideal capacitor (C_{stat}) and FOC connected in series. The apparent compliance expressed in unit of $[\mathrm{l/mmHg}]$ can be written as:

$$C_c^D = \frac{C_{stat}C_\alpha(j\omega)^\alpha}{C_{stat}(j\omega) + C_\alpha(j\omega)^\alpha + RC_\alpha C_{stat}(j\omega)^{\alpha+1}}. \quad (15)$$

5) Model E: It comprises a resistor (R_1) in parallel to a FOC and a resistor (R_2) connected in series. The apparent compliance expressed in unit of $[\mathrm{l/mmHg}]$ can be written as:

$$C_c^E = \frac{1 + (R_1 + R_2)C_\alpha(j\omega)^{\alpha-1}}{R_1(1 + R_2C_\alpha(j\omega)^\alpha)}. \quad (16)$$

B. Integer-order Models

1) Model F: This model correspond to the general apparent compliance-based model for viscoelastic material [25] which is expressed as:

$$C_c^F = C_{stat}\frac{\prod_{n=1}^{N} a_n((j\omega) + b_n)}{\prod_{n=1}^{N} b_n((j\omega) + a_n)}, \quad (17)$$

where a_n and b_n are imperial constants that can be convenient to fit any particular case. C_{stat} denoting the static compliance for the vessel. Goedhard et. all showed that this model could fit an experimental data with N=4. Hence in our comparison we choose N=4.

2) Model G: : It corresponds to the Voigt-cell model that consists of an ideal capacitor, (C_{stat}) accounting for the static compliance in series to a resistor (R_d), accounting for viscous losses.

$$C_c^G = C_{stat}\frac{1}{1 + (j\omega)R_dC_{stat}}. \quad (18)$$

IV. Materials and Method

A. In-vivo human-aging and animal datasets

In order to validate the proposed approach, in this study, we use real data for both human-aging and animal subjects. The *in-vivo* human data was extracted and digitized from aging studies (Nichols et al., [24]). It consists of measured aortic blood flow rate (Q_a) and aortic blood pressure (P_a) at different ages, namely 28, 52, and 68 years. The cardiac beating period for all three subjects is $T = 0.95\ Sec.$ In addition, to further compare and check the efficiency of the proposed models, we utilized animal (pigs and dogs) data extracted and digitized from (Segers et al., [26]).The cardiac beating period for the dog case is $T = 0.46\ Sec$, and for the pig subject is $T = 0.52\ Sec.$ Fig.2 and Fig.3 show the blood flow and pressure signals for each subject that we have used.

B. Parameters fitting of the models

The parameters of the proposed fractional-order representations of the apparent arterial compliance along with the integer ones were estimated by a non-linear least square minimization routine, making use of the well-known $\mathrm{MATLAB-R2020b}$, function *fmincon*. The parameters to estimate for each model's representation C_c^{Model} are refereed as Θ^{Model} where $Model = \{(A),(B),(C),(D),(E),(F),(G)\}$ corresponds to the index of the model's representation: $\Theta^{Model} = \{\Theta^{(A)} = \{C_{\alpha_A}; \alpha_A\},\ \Theta^{(B)} = \{C_{stat_B}; C_{\alpha_B}; \alpha_B\},\ \Theta^{(C)} = \{R_C; C_{\alpha_C}; \alpha_C\},\ \Theta^{(D)} = \{R_D; C_{stat_D}; C_{\alpha_D}; \alpha_D\},\ \Theta^{(E)} = \{R_{1_E}; R_{2_E}; C_{\alpha_E}; \alpha_E\},\ \Theta^{(F)} = \{C_{stat_F}; a_i; b_i; i = 1,2,3,4\},\ \Theta^{(G)} = \{R_d; C_{stat}\}\ \}$ The steps used to obtain the optimal estimates are outlined in Algorithm 1.

C. Statistical Analysis

To examine and compare the ability of the proposed models in reproducing the real apparent arterial compliance, we evaluate the $RMSE$ (step 8 in Algorithm 1). In addition, because the model representations have a different number of parameter, to perform a fair comparison, along with

Algorithm 1 Parameter calibration of the models

1: Load the datasets of the aortic blood pressure ($\mathrm{P_{in}}$) and flow rate (Q)
2: Evaluate the Fast Fourier Transform (FFT) of both P and Q
3: Select the frequency range (Hz) $\mathrm{f} \in [0\ 13]$
4: Calculate the aortic input impedance $\mathrm{Z_{in}}$
▷ Using equation (5)
5: Calculate the in-silico apparent compliance $\mathrm{C_{app}}$
▷ Using equation (7)
6: Select the model to fit with the data
7: Include and Initialize the parameter to estimate Θ
8:

$$\mathrm{RMSE} = \sqrt{\frac{\sum_{\mathrm{i}=1}^{\mathrm{N_s}} \left(\left[\frac{\mathrm{Re} - \hat{\mathrm{Re}}}{\max(\mathrm{Re})} \right]^2 + \left[\frac{\mathrm{Im} - \hat{\mathrm{Im}}}{\max(\mathrm{Im})} \right]^2 \right)}{\mathrm{N_s}}}$$

$$\hat{\Theta} = \arg\min_{\Theta} \ \mathrm{RMSE}$$

% Where $\mathrm{N_s}$ denoting the number of excited frequency points, Re and Im denoting the real and imaginary parts of the real $\mathrm{C_{app}}$, and Im, evaluated in step (5), and $\hat{\mathrm{Re}}$ and $\hat{\mathrm{Im}}$ designate the real and imaginary parts of the model of $\mathrm{C_C^{Model}}(\Theta)$, respectively. $\hat{\theta}$ denotes the estimates that minimize RMSE

the $RMSE$, we evaluate the Bayesian Information Criterion (BIC) and the corrected Akaike Information Criterion (AIC_C) that are defined as follows:

$$\begin{cases} BIC = -2 \cdot ln(RMSE) + P \cdot ln(N_s) \\ \\ AIC_C = -2 \cdot ln(RMSE) + \dfrac{2 \cdot P \cdot N_s}{N_s - P - 1}, \end{cases} \tag{19}$$

where P is the number of parameters.

V. Results & Discussion

The values of the goodness of fit criterion $RMSE$ as well as the calculated {BIC, and AIC_c}, after fitting the human and animal dataset to the proposed fractional-order models and the standard ones, are presented in TABLE I, TABLE II and TABLE III, respectively. Based on these results, it is clear that the fractional-order model representations grant an acceptable reproducing of the real arterial apparent compliance with a minimum number of parameters. The fractional-order *Model (C)* and *Model (E)* present the best RMSE comparing to the other fractional-order models. The comparison between the proposed fractional-order models and the integer models *Model (F)* and *Model (G)* shows that as the models differ in terms of performance, there is a trade-off between the number of parameters per representation (complexity) and accuracy. In fact, complicated configurations offer better RMSE at the cost of the complexity. In order to take into account this compromise, the BIC and AIC criteria have been evaluated. Accordingly, *Model (A)* and *Model (B)* present the minimum values. Overall, using the fractional-order element enhances the accuracy of the arterial compliance and reduces the complexity. For example, approximately the same performances are obtained using both *Model (C)* and *Model (F)*. However, in the representation-based *Model (C)*, only three parameters have been used rather than nine parameters in *Model (F)*.

TABLE IV presents the parameter estimates of the proposed fractional-order models for each human and animal subject. Using *Model (A)* and *Model (B)*, for all the subjects, the fractional-order, α, is less than 1. These results prove that the fractional-order behavior of the apparent compliance. In fact, in this estimation, for the parameter α, we have only constrained the lower bound to be zero; however, for the upper bound, it was unconstrained. Therefore, this effect implies that the vascular system presents a viscoelastic behavior, not a purely elastic one. Indeed, the fact that $\alpha \neq 1$ indicates that the fractional-order element comprises both resistance and capacitance parts, as demonstrated mathematically in Eq. (9). The contributions from both the resistive part and the capacitive one within the fractional-order capacitor are regulated by the fractional power, α, enabling a more flexible physiological description. As the fractional power

TABLE I: $RMSE$ calculated based on the developed fractional-order representation and standard ones for each human-aging and animal subject.

		Model (A)	Model (B)	Model (C)	Model (D)	Model (E)	Model (F)	Model (G)
Human (aging)	68-yr	1.64	1.63	1.51	1.54	1.42	1.16	1.55
	52-yr	1.4	1.38	1.16	1.18	1.1	1.07	1.21
	28-yr	5.44	5.29	2.85	3.96	2.36	2.85	4.31
Animal (healthy)	Pig	1.18	1.14	0.49	0.69	0.45	1.15	0.8
	Dog	20.27	20.12	16.83	18.09	15.22	10.51	18.47

TABLE II: BIC calculated based on the developed fractional-order representation and standard ones for each human-aging and animal subject.

		Model (A)	Model (B)	Model (C)	Model (D)	Model (E)	Model (F)	Model (G)
Human (aging)	68-yr	4.14	4.15	6.87	6.84	9.56	22.79	4.25
	52-yr	4.45	4.49	7.4	7.36	10.06	22.95	4.74
	28-yr	1.74	1.8	5.6	4.94	8.54	20.99	2.21
Animal (healthy)	Pig	3.83	3.9	7.68	6.97	9.9	18.44	4.6
	Dog	-1.86	-1.84	0.59	0.45	2.87	14.01	-1.67

TABLE III: AIC_C calculated based on the developed fractional-order representation and standard ones for each human-aging and animal subject.

		Model (A)	Model (B)	Model (C)	Model (D)	Model (E)	Model (F)	Model (G)
Human (aging)	68-yr	4.34	4.35	8.18	8.14	13.02	107.7	4.45
	52-yr	4.65	4.7	8.7	8.66	13.52	107.87	4.95
	28-yr	1.95	2	6.9	6.25	12	105.9	2.41
Animal (healthy)	Pig	6.67	6.74	15.44	14.73	29.58	-42.28	7.44
	Dog	0.98	1	8.35	8.21	22.55	-46.7	1.17

TABLE IV: Parameter estimates of the fractional-order models for each human-aging and animal subject.

		Model (A)		Model (B)		Model (C)			Model (D)			Model (E)			
Age	Heart rate	C_{α_A}	α_A	C_{stat_B}, C_{α_B}	α_B	R_C	C_{α_C}	α_C	R_D	C_{stat_D}, C_{α_D}	α_D	R_{1_E}	R_{2_E}	C_{α_E}	α_E
Human (aging)	68-yr	2.93	0.2	3.45	0.18	0.14	0.44	1.36	0.12	1.27	1.43	1.8	320	4.41e-5	1.49
	52-yr	3.85	0.34	5.14	0.27	0.08	0.85	1.29	0.07	2.1	1.43	0.88	179.42	2.37e-4	1.25
	28-yr	7.88	0.35	10.65	0.27	0.04	0.92	1.63	0.04	4.36	1.47	0.43	57.17	5.47e-4	1.39
Animal (healthy)	Pig	1.72	0.57	2.59	0.49	0.09	0.25	1.38	0.07	0.87	1.42	2.6	0.24	0.06	1.36
	Dog	3.07	0.28	3.65	0.25	0.12	0.13	1.61	0.1	0.98	1.38	2	728.44	1.94e-5	1.38

increases to 1, the capacitance part dominates and, hence the arterial system behaves like a pure elastic system, and as α approaches to 0, the resistive part increases, and consequently the arterial system acts like a pure viscous system.

By observing the values of the fractional-order differentiation of the *Model (C) Model (D)* and *Model (E)*, it is clear that for all the subjects, this parameter is higher than 1. Functionally, as α exceeds 1, the real part of the fractional-order capacitor impedance, Z_r, becomes negative, and hence it has the characteristic of a negative resistor affording power. Having a negative resistance in these models appears as compensation for the added static resistance in those representations. It is worth mentioning that the interest of constant resistor and/or capacitor in these fractional-order models is to account for the static viscosity and/or elasticity, respectively, while the fractional-order capacitor represents the ability of the arterial vessel to store blood dynamically.

For ease of visualization, we present in Fig. 4 and Fig. 5 the fractional differentiation order estimates, α, of each fractional-order model for the human and animal subject, respectively. From Fig. 4, it is clear that α_A and α_B increase as the age decreases. This result is in coherence with what has been demonstrated in several human-aging studies. In fact, it is well recognized that the arterial vessel becomes stiffer with age. On the other hand, as we explained before, when α goes to 0, the resistive part increases within the fractional-order element, and the system behaves as a viscous element. For the other models based $\{\alpha_C, \alpha_D, \text{and } \alpha_E\}$ where their values exceed 1, we can notice that from 68 years old subject to 52 years old one, the values of α decrease; however, the 28 years old subject presents the highest value. In this case, more real data are needed to affirm such conclusion and correlation between the evolution of the fractional differentiation order and age. In Fig. 5, α_A and α_B of the dog are less than the ones of the pig. By checking the blood pressure waveform of these two animals in Fig. 3, it is clear that the pig's systolic and diastolic blood pressure values are larger than the dog's ones. Accordingly, the results can be interpreted, as the increase of the hemodynamic values might be a consequence of increased vessel stiffness, leading to a decrease in α. For $\{\alpha_C$, which exceeds 1, we notice that α_C of the pig is less than the dog's one, which is consistent with the previous results. However, $\{\alpha_D$ and $\alpha_E\}$ are approximately equal for both animals. The discussed results show the inherent benefits of using fractional-order elements in describing and characterizing the apparent arterial compliance. Fractional-order modeling offers an acceptable accuracy with a minimum number of parameters. The analysis of the variation of the fractional differentiation order in human-aging and animals points out the potential of this parameter to be adopted as a surrogate measure of the arterial stiffness or marker of cardiovascular diseases. The fractional-order might be used to describe the transition between viscosity and elasticity more accurately. Future clinical and experimental validations are required to prove the concept within a wide spectrum of normal and pathological cardiovascular conditions.

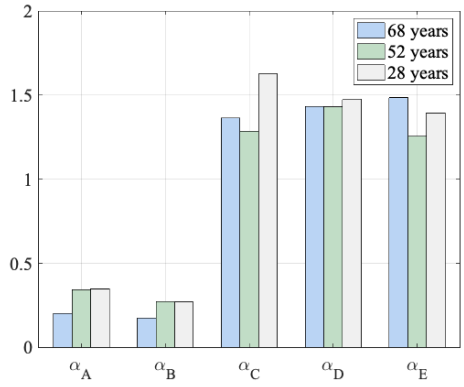

Fig. 4: Estimated fractional differentiation order α using fractional-order models {Model (A), Model (B), Model (C), Model (D), Model (E)} for human-aging.

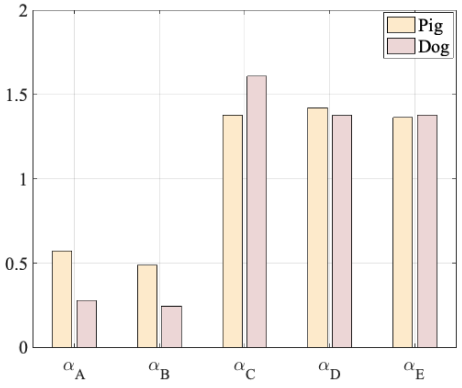

Fig. 5: Estimated fractional differentiation order using fractional-order models {Model (A), Model (B), Model (C), Model (D), Model (E)} for animals (Pigs and Dogs) ones.

VI. Conclusion

Indices and surrogate measurements of arterial compliance present a non-invasive assessment of the vasculature's health and can provide appropriate knowledge about an individual's future risk of morbidity and mortality. The appearance of fractional-order behavior in the arterial system has been identified by many experimental studies of the viscoelasticity properties of the collagenous tissues in the arterial bed; the analyzes of the arterial blood flow and red blood cell membrane mechanics; and the characterizing the heart valve cusp. This paper introduced a fractional-order modeling approach to assess apparent arterial compliance. The models incorporate fractional-order capacitors and ideal resistors and capacitors to display the dynamic relationship between the blood volume and aortic input pressure. The majority of proposed parametric models present reasonable fit performance with *in-vivo* human and animal data. The results show that fractional-order model structures conveniently capture the capacity of the arterial system to store the blood. The fractional-order-based approach of arterial compliance has a great potential to provide a new alternative in assessing arterial stiffness. Future investigations will be directed toward integrating these models within a complete lumped-parameter model for the systemic circulation and study the effects of certain cardiovascular pathologies upon changes in the dynamic arterial compliance represented by the fractional-order capacitor. We provide a publicly available Matlab code used for the numerical implementation and models calibration in this study. The pre-processed data investigated in this study is also available along with the statistical analysis tools. The algorithms and data are available at https://github.com/EMANG-KAUST/Human-and-animal-Fractional-modeling-of-vascular-compliance.

Acknowledgment

Research reported in this publication was supported by King Abdullah University of Science and Technology (KAUST) with the Base Research Fund (BAS/1/1627-01-01).

References

[1] Y. Ruan, Y. Guo, Y. Zheng, Z. Huang, S. Sun, P. Kowal, Y. Shi, and F. Wu, "Cardiovascular disease (cvd) and associated risk factors among older adults in six low-and middle-income countries: results from sage wave 1," *BMC public health*, vol. 18, no. 1, pp. 1–13, 2018.

[2] H. Tanaka, F. A. Dinenno, K. D. Monahan, C. M. Clevenger, C. A. DeSouza, and D. R. Seals, "Aging, habitual exercise, and dynamic arterial compliance," *Circulation*, vol. 102, no. 11, pp. 1270–1275, 2000.

[3] C. M. Quick, D. S. Berger, and A. Noordergraaf, "Apparent arterial compliance," *American Journal of Physiology-Heart and Circulatory Physiology*, vol. 274, no. 4, pp. H1393–H1403, 1998.

[4] N. Westerhof, J.-W. Lankhaar, and B. E. Westerhof, "The arterial windkessel," *Medical & biological engineering & computing*, vol. 47, no. 2, pp. 131–141, 2009.

[5] R. Burattini and S. Natalucci, "Complex and frequency-dependent compliance of viscoelastic windkessel resolves contradictions in elastic windkessels," *Medical engineering & physics*, vol. 20, no. 7, pp. 502–514, 1998.

[6] C. M. Quick, D. S. Berger, D. A. Hettrick, and A. Noordergraaf, "True arterial system compliance estimated from apparent arterial compliance," *Annals of biomedical engineering*, vol. 28, no. 3, pp. 291–301, 2000.

[7] M. A. Bahloul and T. M. Laleg-Kirati, "Three-element fractional-order viscoelastic arterial windkessel model," in *2018 40th Annual International Conference of the IEEE Engineering in Medicine and Biology Society (EMBC)*. IEEE, 2018, pp. 5261–5266.

[8] R. L. Magin, *Fractional calculus in bioengineering*. Begell House Redding, 2006.

[9] C. M. Ionescu, J. T. Machado, and R. De Keyser, "Modeling of the lung impedance using a fractional-order ladder network with constant phase elements," *IEEE Transactions on biomedical circuits and systems*, vol. 5, no. 1, pp. 83–89, 2010.

[10] Y. Kobayashi, A. Kato, H. Watanabe, T. Hoshi, K. Kawamura, and M. G. Fujie, "Modeling of viscoelastic and nonlinear material properties of liver tissue using fractional calculations," *Journal of Biomechanical Science and Engineering*, vol. 7, no. 2, pp. 177–187, 2012.

[11] P. Perdikaris and G. E. Karniadakis, "Fractional-order viscoelasticity in one-dimensional blood flow models," *Annals of biomedical engineering*, vol. 42, no. 5, pp. 1012–1023, 2014.

[12] J. P. Zerpa, A. Canelas, B. Sensale, D. B. Santana, and R. Armentano, "Modeling the arterial wall mechanics using a novel high-order viscoelastic fractional element," *Applied Mathematical Modelling*, vol. 39, no. 16, pp. 4767–4780, 2015.

[13] D. Craiem and R. L. Magin, "Fractional order models of viscoelasticity as an alternative in the analysis of red blood cell (rbc) membrane mechanics," *Physical biology*, vol. 7, no. 1, p. 013001, 2010.

[14] T. C. Doehring, A. D. Freed, E. O. Carew, and I. Vesely, "Fractional order viscoelasticity of the aortic valve cusp: an alternative to quasi-linear viscoelasticity," *Journal of biomechanical engineering*, vol. 127, no. 4, pp. 700–708, 2005.

[15] D. Craiem and R. L. Armentano, "A fractional derivative model to describe arterial viscoelasticity," *Biorheology*, vol. 44, no. 4, pp. 251–263, 2007.

[16] D. Craiem, F. J. Rojo, J. M. Atienza, R. L. Armentano, and G. V. Guinea, "Fractional-order viscoelasticity applied to describe uniaxial stress relaxation of human arteries," *Physics in Medicine & Biology*, vol. 53, no. 17, p. 4543, 2008.

[17] M. A. Bahloul and T. M. Laleg-Kirati, "Arterial viscoelastic model using lumped parameter circuit with fractional-order capacitor," in *2018 IEEE 61st International Midwest Symposium on Circuits and Systems (MWSCAS)*. IEEE, 2018, pp. 53–56.

[18] M. A. Bahloul and T.-M. L. Kirati, "Fractional-order model representations of apparent vascular compliance as an alternative in the analysis of arterial stiffness: an in-silico study," *Physiological Measurement*, vol. 42, no. 4, p. 045008, 2021.

[19] M. A. Bahloul and T.-M. Laleg-Kirati, "Assessment of fractional-order arterial windkessel as a model of aortic input impedance," *IEEE Open Journal of Engineering in Medicine and Biology*, vol. 1, pp. 123–132, 2020.

[20] M. A. Bahloul and T.-M. L. Kirati, "Two-element fractional-order windkessel model to assess the arterial input impedance," in *2019 41st Annual International Conference of the IEEE Engineering in Medicine and Biology Society (EMBC)*. IEEE, 2019, pp. 5018–5023.

[21] M. Nakagawa and K. Sorimachi, "Basic characteristics of a fractance device," *IEICE Transactions on Fundamentals of Electronics, Communications and Computer Sciences*, vol. 75, no. 12, pp. 1814–1819, 1992.

[22] M. S. Semary, M. E. Fouda, H. N. Hassan, and A. G. Radwan, "Realization of fractional-order capacitor based on passive symmetric network," *Journal of advanced research*, vol. 18, pp. 147–159, 2019.

[23] G. Ala, M. Di Paola, E. Francomano, Y. Li, and F. P. Pinnola, "Electrical analogous in viscoelasticity," *Communications in Nonlinear Science and Numerical Simulation*, vol. 19, no. 7, pp. 2513–2527, 2014.

[24] W. Nichols, "Effects of age and of hypertension on wave travel and reflections," *Arterial vasodilation: Mechanisms and therapy*, 1993.

[25] W. Goedhard and A. Knoop, "A model of the arterial wall," *Journal of biomechanics*, vol. 6, no. 3, pp. 281–288, 1973.

[26] P. Segers, N. Stergiopulos, N. Westerhof, P. Wouters, P. Kolh, and P. Verdonck, "Systemic and pulmonary hemodynamics assessed with a lumped-parameter heart-arterial interaction model," *Journal of engineering mathematics*, vol. 47, no. 3, pp. 185–199, 2003.